JOURNAL OF GEOPHYSICAL RESEARCH, VOL. 105, NO. C11, PAGES 26,167–26,177, NOVEMBER 15, 2000

Annual cycle of the Brazil-Malvinas confluence region in the National Center for Atmospheric Research Climate System Model

Ilana Wainer

Department of Physical Oceanography, University of São Paulo, Brazil

Peter Gent

National Center for Atmospheric Research, Boulder, Colorado

Gustavo Goni

Atlantic Oceanographic and Meteorological Laboratory, National Oceanic and Atmospheric Administration, U.S. Department of Commerce, Miami, Florida

Abstract. The objective of this study is to compare the mean and seasonal variability of the circulation in the southwest Atlantic with observations. The results used in the comparison are from the last 200 years of a 300 year control integration of the Climate System Model (CSM). The area of study includes the confluence region between the subtropical and subpolar waters represented by the Brazil and Malvinas Currents. The seasonal variation of transport and its relationship to changes in the wind stress forcing and in the sea surface temperature are examined and compared to available oceanographic observations. This study shows that a coarse resolution climate model, such as the CSM, can successfully reproduce major characteristics of the Brazil-Malvinas confluence seasonality, although the mesoscale features involving recirculation and meander dynamics are not resolved. The CSM transport values in the region of 38°S are consistent with hydrographically derived values. The transport of the CSM Brazil Current is higher during austral summer and smaller during austral winter. Conversely, the Malvinas Current transport is weaker during austral summer and stronger during austral winter. This is also consistent with observations. The CSM seasonal cycle in transport associated with both the Brazil and Malvinas Currents and its meridional displacement is closely linked to the seasonal variations in the local wind stress curl. However, the displacement is much smaller in the model than in observations. The CSM results show that the latitudinal displacement of the 24°C and 17°C at the South American coast beween austral summer and winter is 20° and 12°, respectively. This is very similar to the displacement seen in observations.

1. Introduction

The Brazil-Malvinas confluence region (hereafter referred to as the BMC) is one of the most enegetic regions of the world ocean [*Chelton et al.*, 1990]. It is a frontal zone formed by the merging of the southward flowing, warm, and salty Brazil Current and the northward flowing, cold, and relatively fresh Malvinas Current (also known as the Falklands Current).

The behavior of the confluence on a broad range of temporal scales and the interaction of this behavior with climate variability have been subjects of growing interest. Several studies [*Gordon* and *Greengrove*, 1986; *Roden*, 1986; *Reid*, 1989; *Garzoli* and *Garraffo*, 1989; *Gordon*, 1989; Confluence Principal Investigators, 1990; *Garzoli* and *Simonato*, 1990; *Maamaatuaiahutapu* et al., 1992; *Provost et al.*, 1992; *Garzoli*, 1993; *Matano et al.*, 1993; *Garzoli* and *Giulivi*, 1994; *Goni et al.*, 1996] have examined the dynamics of the BMC region at annual and shorter timescales.

Typically, the Brazil Current separates from the coast and veers offshore together with the Malvinas Current at about 36°S. The line of confluence close to the coast is oriented almost parallel to the shore and is usually considered to be located near the shelf break [*Olson et al.*, 1988]. The confluence shows strong seasonal fluctuations, moving from 40°-46°S during summer [*Legeckis* and *Gordon*, 1982] to as far north as 35°-30°S during winter [*Ciotti et al.*, 1985]. *Olson et al.* [1988] showed, based on drifter and satellite observations, that the latitude of the separation of the Brazil Current from the continental shelf (hereafter referred to as latitude of separation) is subject to very strong seasonal variations, being farther north in austral winter (July and August), and farther south in austral summer (January and February).

The mean separation latitude of the Brazil Current, approximately 36°S, is observed to occur nearly 10° north of the climatological zero line in wind stress curl [*Matano*,

Paper number 1999JC000134.
0148-0227/00/1999JC000134$09.00

1993]. This situation has been explained in terms of its encounter with the northward flowing Malvinas Current [*Veronis*, 1973; *Matano*, 1993; *Agra* and *Nof*, 1993]. The hypothesis is that this stronger subpolar boundary current, approximately 70 Sv [*Peterson*, 1992], essentially prevents the Brazil Current from flowing further south. Understanding the dynamics of the two colliding currents is essential to explaining the temporal variability of the separation latitude.

These relatively recent results indicate that the southern and northern limit of the confluence may depend on the mass transport of both the Brazil and Malvinas Currents [*Matano*, 1993; *Agra* and *Nof*, 1993] and on local wind forcing [*Garzoli* and *Giulivi*, 1994]. Geostrophic velocities in the BMC region were computed by *Garzoli* [1993], based on data obtained by an array of inverted echo sounders deployed as a part of the International Confluence Program [*Confluence Principal Investigators*, 1990]. Using data from ship surveys conducted under the same program, *Maamaatuaiahutapu et al.* [1992] investigated the water mass composition at the confluence. The variability of the sepation of the Brazil and Malvinas Currents from the shelf break leads to large sea surface temperature (SST) variations both on seasonal and interannual timescales. Based on infrared satellite imagery, *Provost et al.* [1992] analyzed the temporal variability of SST in the region and found that in most cases, it can be accurately described by the annual and semiannual modes, and that the annual SST mode weakens to the south. The predominant modes were shown to be tied to the relative strengths of the annual cycle in the Brazil Current, which is forced by winds in the subtropics, and the semiannual cycle in the Antartic Circumpolar Current (ACC), which is forced by the winds at the Drake Passage.

Pulses in the zonal wind component across the Drake Passage can be related to pulses in the ACC [e.g., *Peterson*, 1992; *Garzoli* and *Giulivi*, 1994]. Because the Malvinas Current is part of the ACC, its northward penetration could be associated with these wind events. However, the study of *Garzoli* and *Giulivi* [1994] shows that the main source of variability of the confluence front is the local wind forcing, and there is no apparent correlation between wind-forced pulses in the ACC and the observed northward penetration of the Malvinas Current. These results are directly concerned with wind forcing, but there are several other factors that may modify these annual and semiannual signals to produce interannual variability.

The objective of this study is to examine and validate against observations the mean climatology and seasonal cycle of the southwest Atlantic and the BMC in the Climate System Model (CSM). The seasonal variation of transport and its relationship to changes in the wind stress forcing and in the SST will be examined and compared to available oceanographic observational data products, which are described below.

2. Model Description and Observed Data Sets

The CSM is a coupled, global general circulation ocean-atmosphere-land and sea ice model developed at the National Center for Atmospheric Research (NCAR) [*Boville* and *Gent*, 1998]. The atmospheric component of this model is the Community Climate Model, version 3 with T42 resolution (approximately 2.8° in latitude and longitude with 18 vertical layers). Details about the atmospheric component have been given by *Kiehl et al.* [1998] and *Hack et al.* [1998]. The ocean component of this model was developed from the Geophysical Fluid Dynamics Laboratory z coordinate primitive equation model [*Gent et al.*, 1998]. The spatial resolution is 2.4° in longitude, with variable resolution in latitude ranging from 1.2° to 2.3° and 45 vertical levels. The meridional resolution is 2.2° at 20°S and 1.8° at 40°S. The sea ice model dynamics is the cavitating fluid rheology of *Flato* and *Hibler* [1992], and it is described by *Weatherly et al.* [1998]. The land surface model allows for different vegetation types and is described by *Bonan* [1998]. Although the land surface model computes river runoff, it is not transferred to the ocean model. The interaction between river runoff and shelf processes, a significant problem of human-scale relevance, has now been implemented in a later version of the coupled model.

The model data analyzed are monthly mean output from the last 200 years of a 300 year control run of the CSM [*Boville* and *Gent*, 1998]. Model results for 40°S, within the BMC region, are then compared to the surface climatological fields from the National Center for Environmental Prediction (NCEP) atmospheric reanalysis project [*Kalnay et al.*, 1996]. The annual climatologies of *Hellerman* and *Rosenstein* [1983] (HR) and *Oberhuber* [1988] (OBER) are used when comparing BMC region wind stress. The OBER data product contains climatological monthly means of heat fluxes and radiation budgets over the global oceans, based on analyses of the Comprehensive Ocean-Atmosphere Data Set (COADS), as documented by *Slutz et al.* [1985] and *Woodruff et al.* [1987], for the period 1950 - 1979. Further comparison of the CSM model results is made with the 1945 - 1989 climatology of *DaSilva et al.* [*DASILVA*, 1994], this data set is also based on COADS, but has improved resolution and boundary layer parameterizations, including a new scientific Beaufort equivalent scale, which reduces wind speed bias and artificial wind speed trends. CSM SSTs are also compared to the *Reynolds* and *Smith* [1994] climatology, which was constructed using sea surface temperature fields blended from ship, buoy, and bias-corrected satellite data.

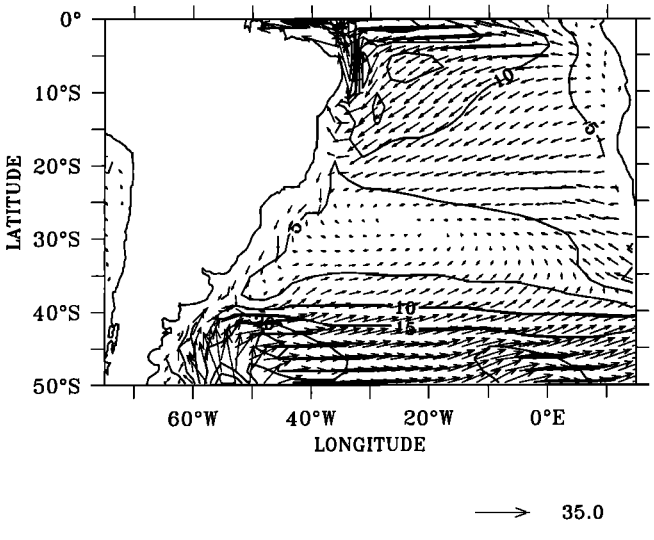

Figure 1. Climate System Model (CSM) annual mean surface currents. Maximun vector length is 35 cm s^{-1}; velocity magnitude contour interval is 5 cm s^{-1}.

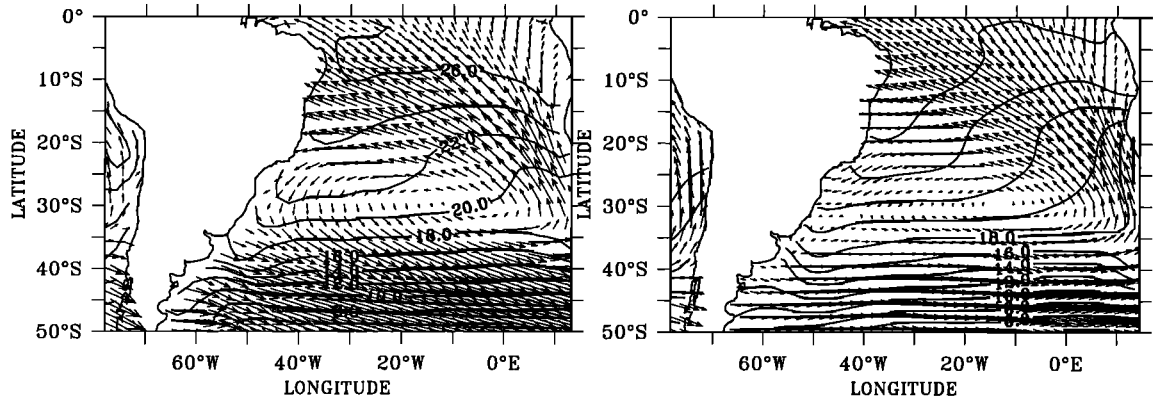

Figure 2. Annual mean wind stress and sea surface temperature (SST) contours from (a) the CSM and (b) *DASILVA et al.* [1994] (*DASILVA*). Maximum vector is 0.15 N m^{-2}, and contour interval is 2°C. In Figure 2b, only every other vector is plotted for clarity.

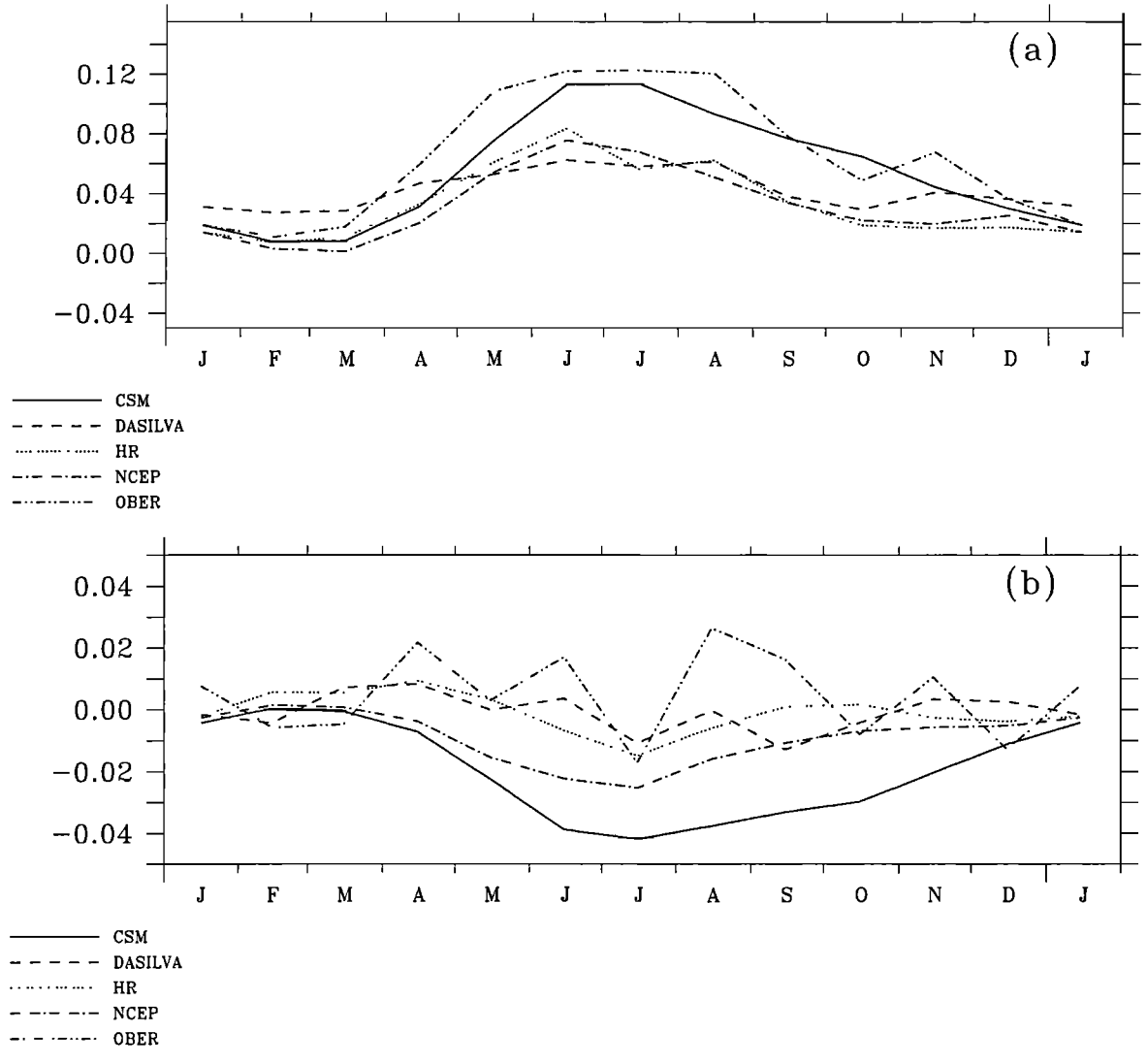

Figure 3. (a) Zonal and (b) meridional components of wind stress, zonally averaged between 65°W and 15°E, at 35°S (N m-2) from the CSM and the *DASILVA*, *Hellerman* and *Rosenstein* [1983] (HR), National Center for Environmental Prediction (NCEP), and *Oberhuber* [1988] (OBER) climatologies.

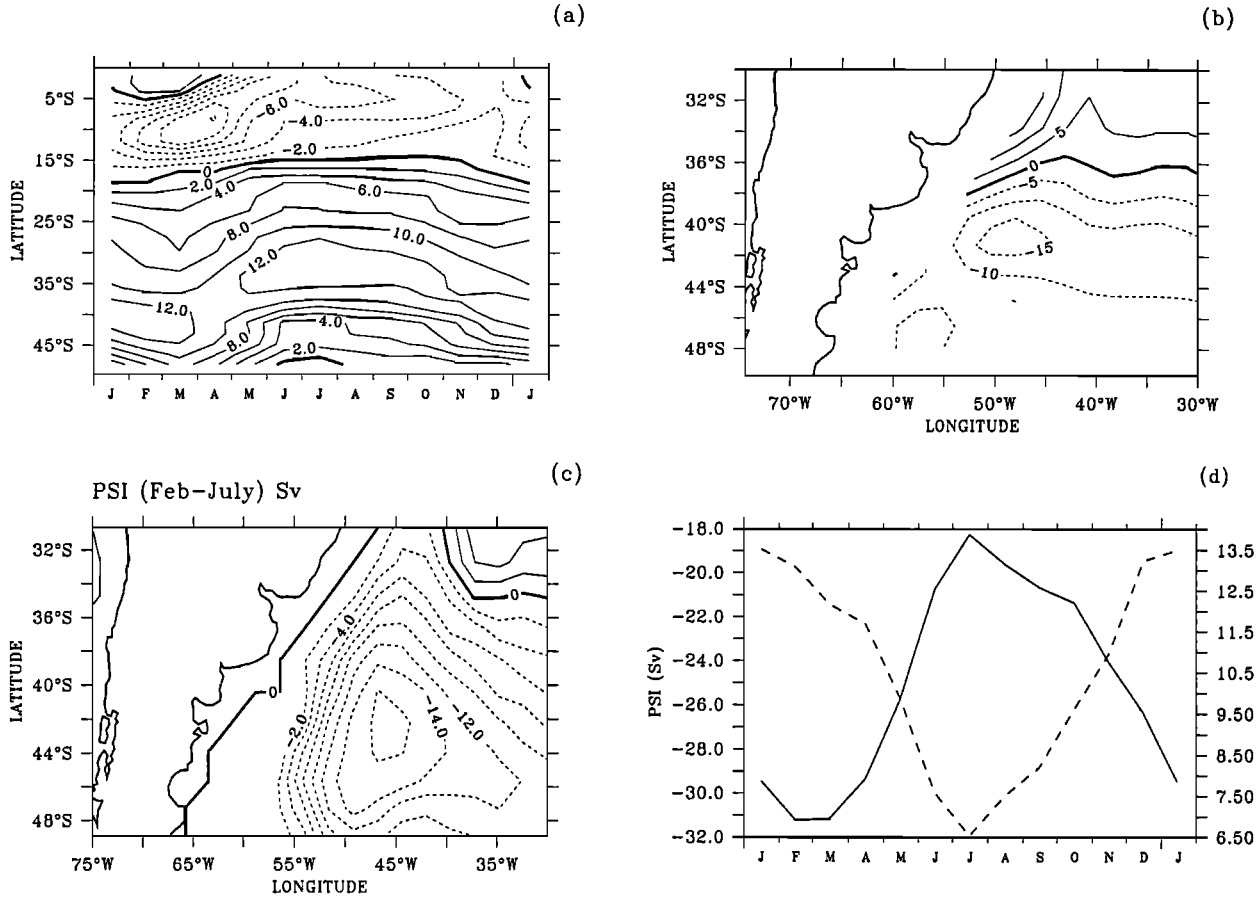

Figure 4. (a) Zonal average between 65°W and 45°W of the CSM wind stress curl (10^{-7} N m^{-3}) as a function of latitude and month, (b) differences between the February and July mean wind stress curl (10^{-7} N m^{-3}), (c) differences between the February and July mean barotropic stream function (Sv), and (d) zonal-averaged wind stress curl (10^{-7} N m^{-3}, dashed line, scale on the right-hand side of the plot), together with the barotropic stream function (Sv, solid line, scale on the left) at the South American coast at 40°S.

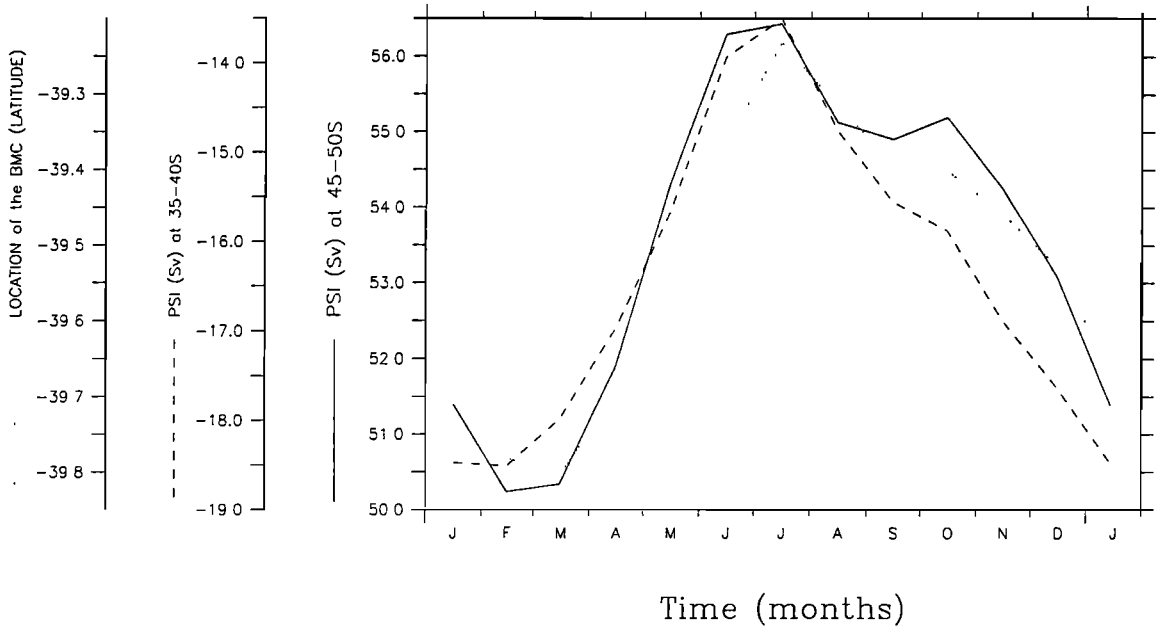

Figure 5. Zonal average between 65°W and 45°W of the CSM barotropic stream function (Sv) averaged between 35° and 40°S (dashed line) and 45°-50°S (solid line) plotted against time of year. The BMC separation point, defined as where the barotropic stream function is zero at the South American coast, is also plotted (dotted line).

3. Results

3.1. Annual Mean Circulation

The dominant feature of the South Atlantic simulated annual mean surface currents in the CSM (Figure 1) is the broad subtropical gyre. Within this gyre, four different regions can be observed: (1) the westward South Equatorial Current in the northern part of the domain, (2) the southward Brazil Current to the west, (3) the eastward South Atlantic Current to the south and (4) the northward Benguela current to the east. This description is in agreement with the wind-driven schematic representation of the currents by *Peterson* and *Stramma* [1991].

The mean annual SSTs from both the CSM (averaged over 200 years) and COADS are shown in Figures 2a and 2b, respectively. They both show a weak southwest-northeast gradient north of 35°S, whereas the isotherms are predominantly zonal further south. This characteristic is also found in the *Reynolds* and *Smith* [1994] SST climatology. Figure 2a also shows the CSM annual mean wind stress in newtons per square meter and Figure 2b shows the observed DASILVA wind stress climatology (1945-1989). The Figure shows that although the overall broad gyre wind circulation patterns are very similar, the wind stress derived from the model is stronger. In fact, the CSM annual mean zonal wind stress component (not shown) is almost twice the value of the DASILVA climatology, except approximately 3° either side of the zero line. The meridional component of the wind stress in the CSM is also stronger, in particular beween 20°W and 15°E, where differences are of the order of 0.03 N m^{-2}. The global annual mean CSM wind stress is also stronger compared to the NCEP reanalysis product [*Danabasoglu*, 1998].

In fact, *Danabasoglu* [1998] concluded that the differences between the CSM results and several observed climatologies are comparable to the differences between the climatological products themselves. To illustrate this point, the components of wind stress at 35°S, zonally averaged between 65°W and 15°E, from the CSM and four other climatologies (DASILVA, HR, NCEP, and OBER) are plotted in Figure 3. From December to March the zonal components of wind stress (Figure 3a) from three data sets and from the CSM are very similar. The only exception in the DASILVA climatology, which shows a stronger zonal stress and has by far the smallest seasonal variation of all the climatologies. From April to July-August there are differences in magnitude, particularly between the CSM and OBER on the high end (maximum values between 0.1 and 0.12 N m^{-2}) and the other three climatologies (maximum values between 0.07 and 0.085 N m^{-2}). OBER has a secondary maximum in the zonal wind

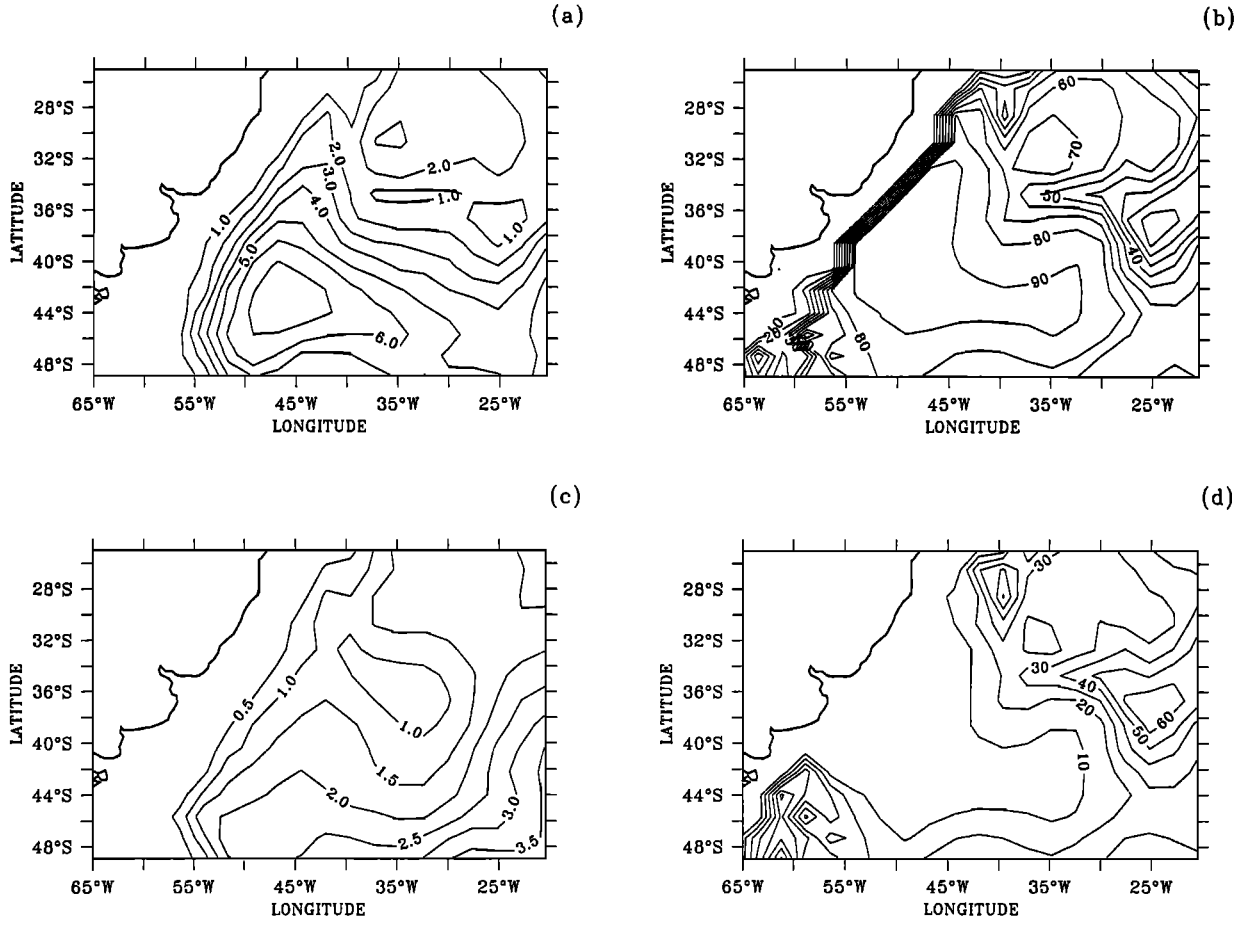

Figure 6. Amplitude of the (a) annual (H1) and (c) semiannual (H2) harmonic of the barotropic stream function (Sv). Percentage of the explained variance of the (b) annual (H1) and (d) semiannual (H2) harmonic of the barotropic stream function.

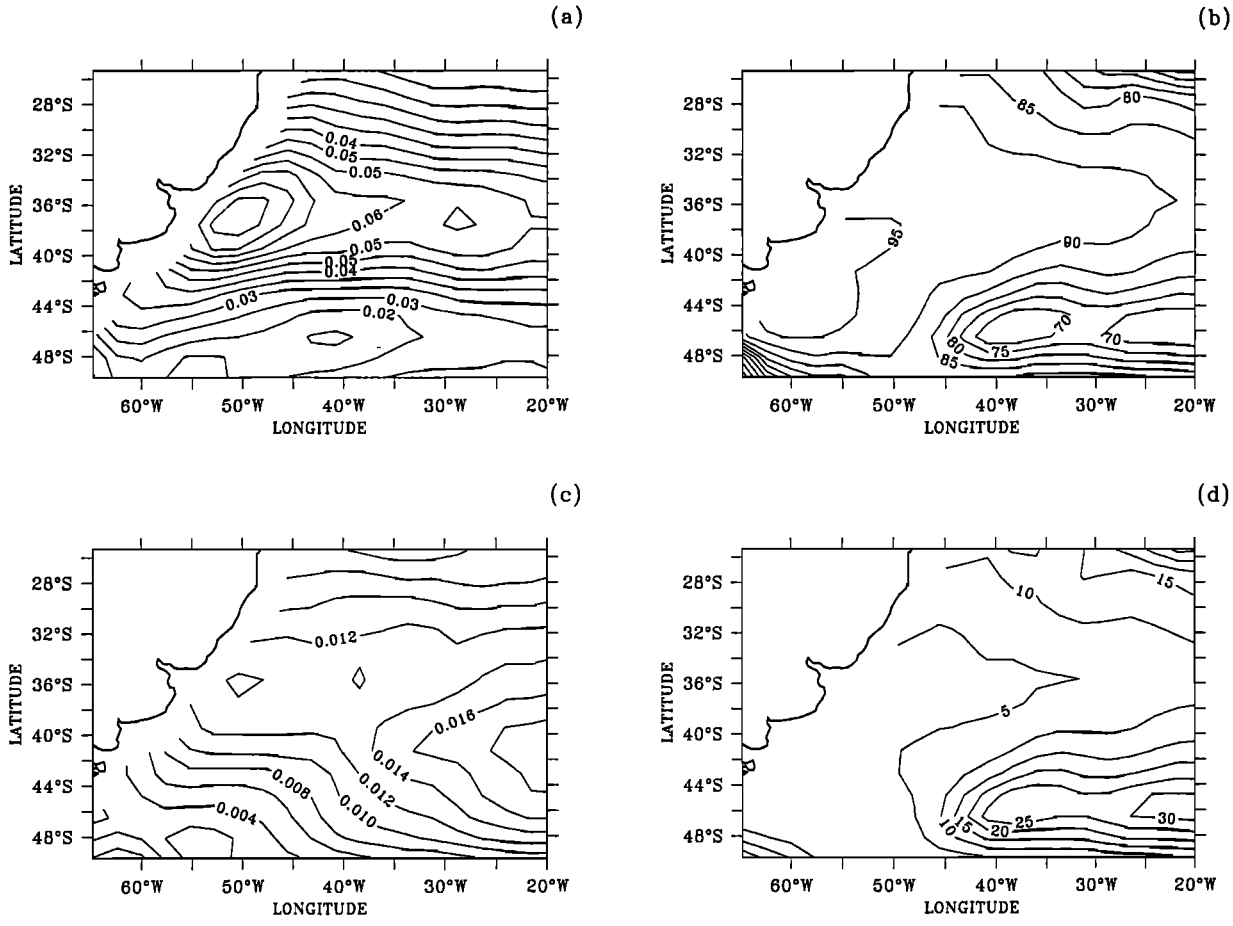

Figure 7. Amplitude of the (a) annual (H1) and (c) semiannual (H2) harmonic of the zonal wind stress (N m-2). Percentage of the explained variance of the (b) annual (H1) and (d) semiannual (H2) harmonic of the zonal wind stress.

stress in November, and HR has a weak secondary maximum in August coincident with the values of DASILVA for the same month. These features do not appear in the CSM or NCEP zonal wind stresses.

The differences between the observed data sets and the CSM meridional component of wind stress are significant (Figure 3b). In particular, OBER and DASILVA exhibit considerable temporal variability, whereas HR, NCEP, and the CSM show a nearly sinusoidal annual cycle with a maximum in July (northerlies) and a minimum in January. The seasonal variation in these last three data sets is considered to be more realistic, but the amplitude of the CSM stress is considerably larger. Section 3.2 analyzes the seasonal cycle of the CSM simulation results, focusing on the BMC region. The main objective of this work is to verify how well the CSM captures the strong seasonal variation associated with the BMC described in section1, both in the wind forcing and in the mass transport associated with the Brazil and Malvinas Currents.

3.2. Seasonal Cycle

3.2.1. Transport and wind stress curl. It is not known precisely what causes the seasonal changes in the location of the separation from the shelf break of the Brazil-Malvinas Currents. One hypothesis is that changes in the South Atlantic wind stress are responsible for the north-south variability of the BMC. Therefore the wind stress curl, zonally averaged between 65°W and 45°W, from the climatology obtained from the last 200 years of the CSM integration is shown as a function of latitude and month in Figure 4a. The annual cycle of the wind stress curl exhibits a dependence on latitude. The seasonal variation of the wind stress curl at lower latitudes in the CSM is dominated by the annual cycle. For example, between the equator and 15°S, the absolute maximum (negative) wind stress curl occurs in April, and the minimum values occur during December. Between 15°S and 35°S, the absolute maximum wind stress curl occurs during June-July, with a minimum in March. Thus the wind stress curl at these latitudes has an important semiannual component. South of 35S, the annual cycle again dominates the wind stress curl variability in the CSM. The seasonal cycle of the wind stress curl has a maximum during austral winter and a minimum during austral summer. Both the Brazil and Malvinas Currents show a strong annual signal in transport in the CSM, suggesting that the variations of the BMC are forced predominantly by transport changes associated with the wind stress curl variability.

The differences between the CSM February and July mean wind stress curl and barotropic stream function are shown in Figures 4b and 4c. The largest change in transport between these two extremes of the seasonal cycle is 16 Sv centered around 42°S. This is also the location of the largest change in wind stress curl. Figure 4c shows that there are slightly larger

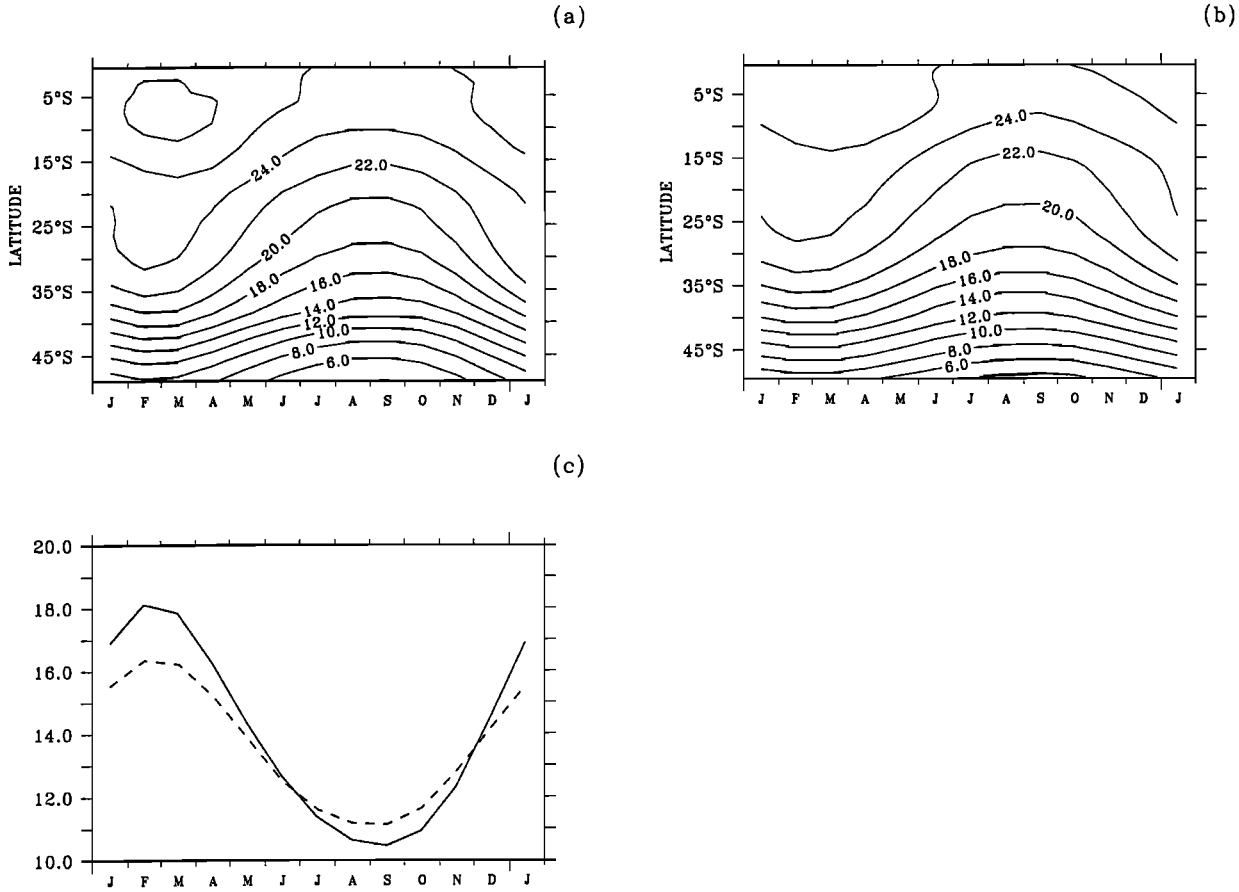

Figure 8. Comparison of the annual cycle of SST, zonally averaged between 65°W and 15°E, for (a) the CSM climatology and (b) the *Reynolds* and *Smith* [1994] climatology. Contour interval is 2°C. Comparison of (c) the zonally averaged SST (°C) climatologies at 40°S; CSM is denoted by the solid line and *Reynolds* and *Smith* [1994] by the dashed line.

changes in the Malvinas Current than in the Brazil Current. This result differs from previous work [*Olson et al.*, 1988], which suggests that differences in the separation are due primarily to annual changes in the Brazil Current, and secondarily to annual changes in the Malvinas Current.

Figures 4b and 4c show that the circulation in the BMC region is highly correlated with the wind stress curl from 35°S to 45°S. This is quantified in Figure 4d, where the wind stress curl, zonally averaged between 65°W and 45°W, is shown (scale on the right) together with the barotropic stream function at the South American coast (Sv, scale on the left) at 40°S. There is a pronounced annual cycle in both the wind stress curl and the barotropic stream function. The correlation coefficient between them is -0.91. A maximum transport value of 31 Sv is found in February-March, with a minimum value of 18.5 Sv in June. These values are consistent with the transport estimates obtained by *Matano* [1993]. They also agree with hydrographic and inverted echo sounder data near 38°S, obtained by *Gordon* and *Greengrove* [1986], *Gordon* [1989], and *Garzoli* and *Garraffo* [1989], which vary between 19 and 22 Sv depending on the time of year. Values obtained from Geosat data by *Goni et al.* [1996] vary between 0 and 40 Sv. However, their results show a more complicated annual cycle than an almost pure first harmonic.

The zonal average of the barotropic stream function between 65°W and 45°W, at 35°-40°S and 45°-50°S (Figure 5), shows that the transport of the simulated Brazil Current is stronger during austral summer and weaker during austral winter. Conversely, the Malvinas Current transport is weaker during summer and stronger during winter. Figure 5 also shows the seasonal cycle of the separation point as a function of latitude (dotted line), defined as where the barotropic stream function is zero at the South American coast. This has been estimated by linear interpolation of the stream function values next to the coast. The Figure shows that the seasonal oscillation of the confluence is directly related to transport changes of the two currents. Although the variation in latitude is small, it is in phase with the transports of both the Brazil and Malvinas Currents. The length of the model control integration makes this small change in latitude significant, but this displacement in the model is much smaller than in observations.

Smith et al. [1994] and *Olson et al.* [1988] showed that the observed variability of the excursions of the two currents along the coast is predominantly annual for the Brazil Current and semiannual for the Malvinas Current. According *to Olson et al.* [1988], the Malvinas Current separation has a semiannual peak that is also seen in altimeter signals and is likely to be a result of semiannual atmospheric forcing over the Southern Ocean.

To better evaluate the role of the annual and semiannual components of the annual cycle in the CSM, a harmonic

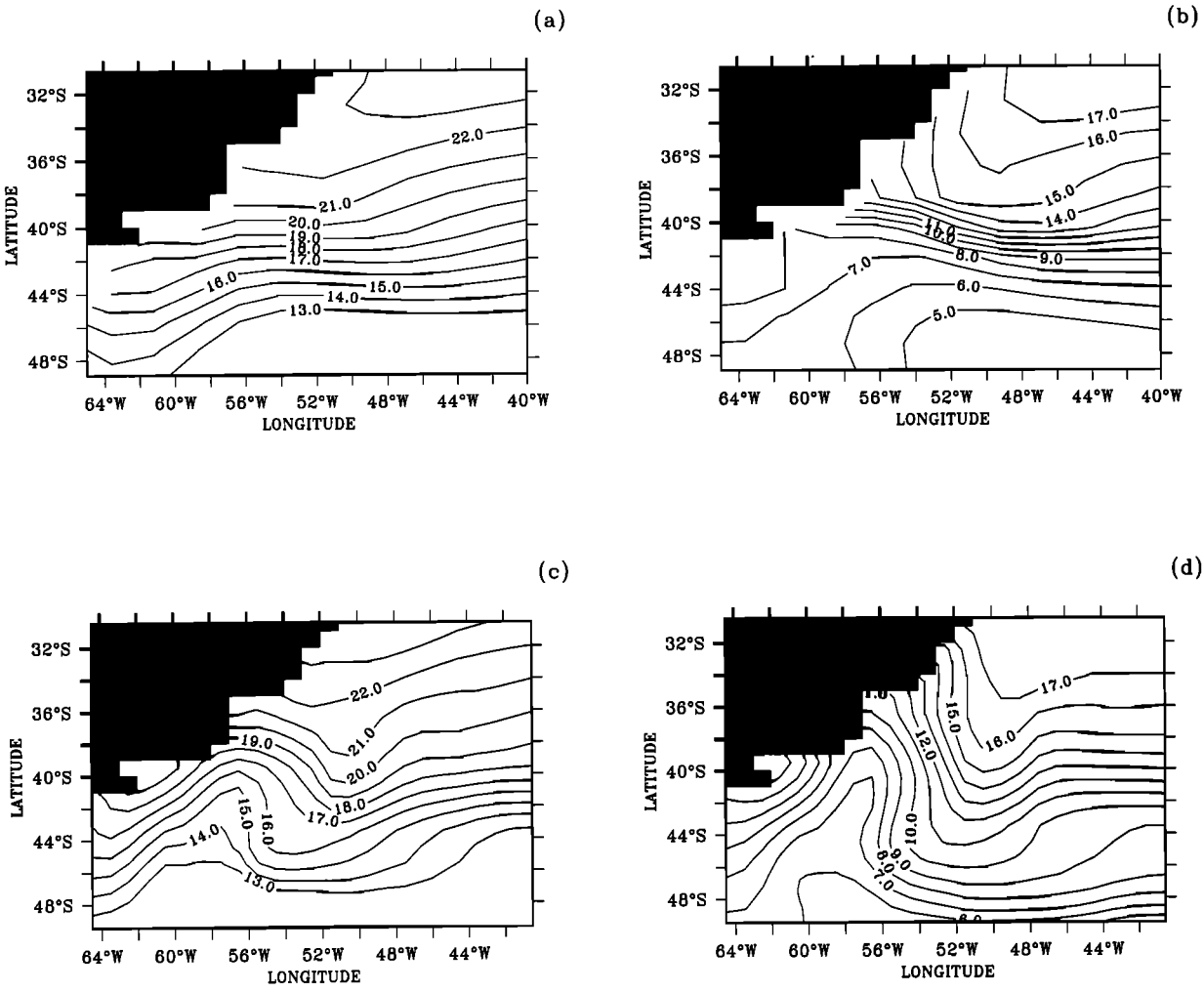

Figure 9. Climatological SST (°C) for the months of (a) January and (b) July at the southwest edge of the South Atlantic region from the CSM and for the mont. of (c) January and (d) July for the same fields, but from the *Reynolds* and *Smith* [1994] climatology.

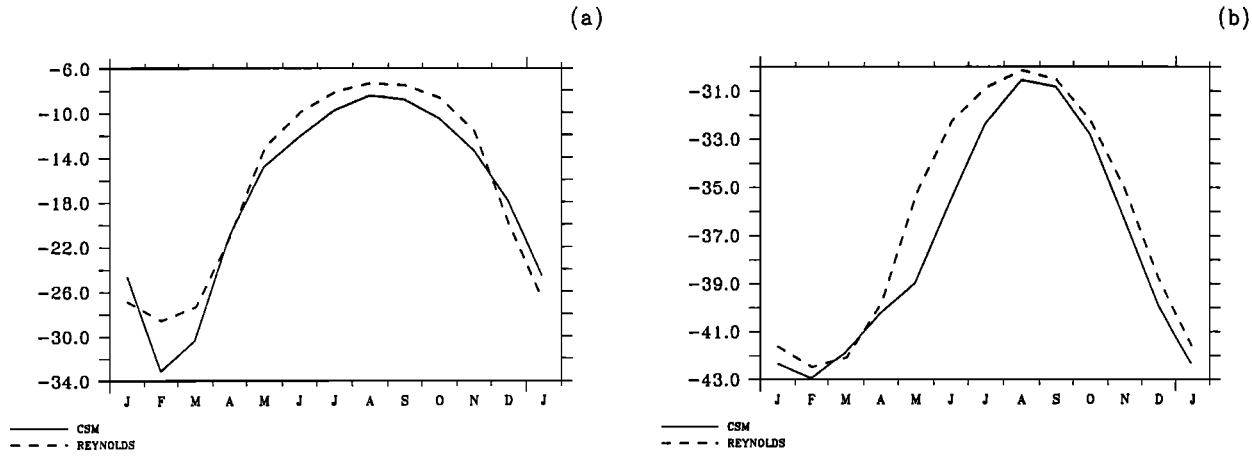

Figure 10. Variation with latitude and time of year of (a) the 24°C and (b) the 17°C isotherms at the South American coast from the CSM (solid line) and *Reynolds* and *Smith* [1994] dashed line.

analysis of the wind stress and barotropic stream function was performed. The amplitude and percentage of the variance explained by the first (H1) and second (H2) harmonics show that the region of study can be accurately described by the sum of the annual and semiannual components. In a large part of the basin the annual harmonic accounts for over 80% of the variability for the barotropic stream function (H1, Figures 6a and 6b), with the exception of the southwest and east areas in the region of study. The highest values of the explained variance (over 60%) of the second harmonic (H2, Figures 6c and 6d) are found south of 40°S, centered at 62°W, associated with the Malvinas Current semiannual peak reported *by Olson et al.* [1988] and at 38°S, 25°W, which is the approximate location where part of the South Atlantic Current recirculates back to the west [*Peterson* and *Stramma*, 1991, Figure 1]. Examination of the explained variances of the first (H1) and second (H2) harmonics of the annual cycle of the zonal wind stress component (Figure 7) shows the dominance of the annual harmonic. The semiannual harmonic explains the remaining variance (less than 20%) in a small region at the very southwest edge of the domain and approximately 30% in the region south of 42°S and east of 45°W. The same analysis for the meridional component (not shown) corroborates the dominance of H1. It is interesting to note that in this case, the highest values of the explained variance of H2 are away from the Malvinas Current region near the coast and well into the central part of the South Atlantic.

3.2.2. Sea surface temperature. Comparison of the annual cycle of SST, zonally averaged between 65°W and 15°E, from the CSM and *Reynolds* and *Smith* [1994] climatologies is shown in Figures 8a and 8b. The phase of the annual cycle is the same in both, with maximum temperatures at the end of summer (February-March) and minimum temperatures at the end of winter (August-September). The same phase of the annual cycle also appears in the DASILVA climatology (not shown). Both zonally averaged climatologies at 40°S are shown in Figure 8c. The phases of the annual cycle are remarkably similar for the model and observations. However, there is a difference in magnitudes: The CSM is 1.5°C warmer than the values reported by *Reynolds* and *Smith* [1994] in February, and in September-October the CSM is approximately 0.5°C colder. This larger-amplitude annual cycle of SST in the CSM might well be caused by the stronger than observed annual cycle of wind stress, which is shown in Figure 2.

The mean SSTs for the months of January and July from the CSM are show in Figures 9a and 9b, and corresponding values from *Reynolds* and *Smith* [1994] are shown in Figures 9c and 9d. The figure shows that the model SST fields are predominantly zonal, whereas the observations show considerable meridional excursions of the isotherms, especially in July. However, the positions of the zonally averaged isotherms are obtained quite well in the CSM (Figure 8). The largest error is located south of 44°S and east of 56°W in July, where the model SST is too cold. The *Reynolds* and *Smith* [1994] climatology shows that in July (Figure 9d), when the Malvinas Current is strong, there is a considerable northward displacement of the isotherms near the coast. This northward displacement is weaker in January (Figure 9c), when the Malvinas Current is weak. The CSM is not able to resolve the local dynamics adjacent to the coast, and a much smaller coastal displacement of the isotherms occurs in the model than in observations.

Figure 10 shows the variation with latitude and time of year of the 24°C isotherm (Figure 10a) and the 17°C isotherm (Figure 10b) at the South American coast from the CSM and the *Reynolds* and *Smith* [1994] climatology. The 24°C isotherm is much further north in austral winter, when it can reach 8°S, and its southernmost position is 29°S in austral summer in the *Reynolds* and *Smith* [1994] climatology. Results from the CSM show that the 24°C isotherm varies between 9°S and 33°S, with very good phase agreement compared to observations. The northernmost location of the 17°C isotherm is 30°S in both the CSM and the *Reynolds* and *Smith* [1994] climatology, while its southernmost location is 42°S in the observations and 43°S in the CSM, again with good agreement in phase. Both the observations and model results show the range of the latitudinal displacement to be about 20° (Figure 10a) and 12° (Figure 10b), for the 24°C and 17°C isotherms, respectively.

4. Comparison With Previous Modeling Studies

We now compare the CSM results to previous ocean alone numerical model studies. *Matano et al.* [1993] investigated the fluctuations of the Brazil and Malvinas Currents using a primitive equation barotropic model forced by climatological wind fields. This work concluded that the latitudinal variation of the BMC is primarily related to changes in the transports of the Brazil and Malvinas Currents, as shown in the present work. Our results also agree with both the numerical model simulation and Geosat altimeter data analysis presented by *Matano et al.* [1993], which show that both the Brazil and Malvinas Currents undergo a similar annual cycle, but with opposite phases.

Results for the seasonal variation of transport within the BMC in the numerical studies of *Smith et al.* [1994], where a wind-driven isopycnic coordinate model is used, show that there is a significant semiannual period associated with the Malvinas Current transport, which does not appear in the CSM. The reason is that the coupled model winds are predominantly annual throughout the southern Atlantic Ocean and results from the CSM ocean component tend to be like linear theory, with midlatitude transports dictated by Sverdrup dynamics [*Danabasoglu*, 1998].

The reason for this linear behavior is that the CSM is not eddy-resolving, and cannot resolve coastal processes within the confluence involving recirculation and meander dynamics. Therefore neither inertia nor topography strongly influence the separation of the Brazil and Malvinas Currents from the coast in the CSM. However, the CSM result agrees with Matano [1993], who used a primitive equation model with higher horizontal resolution of 0.5° to 1°. *Matano* [1993] also concluded that the location of the BMC is governed primarily by the transport of the Malvinas Current.

In a numerical study using a higher-resolution model, forced by observed monthly mean wind stresses, *Gan et al.* [1998] suggested that the time dependence of their imposed Drake Passage transport is what plays the dominant role in establishing the seasonal variability associated with the Brazil and Malvinas Current separation latitude. In the CSM it is not possible to single out this effect on the variability of the Brazil and Malvinas Current separation latitude, but like the results of *Gan et al.* [1998], the predominant timescale is seasonal. Furthermore, as mentioned in section 1, *Garzoli* and *Giulivi* [1994] showed that the main source of variability of the

confluence front is the local wind forcing, with no apparent correlation between wind-forced pulses in the region of Drake Passage.

5. Summary and Conclusions

The annual mean and seasonal variabilities of the southwest Atlantic circulation have been investigated using the NCAR CSM. The mean and annual cycle climatologies from the last 200 years of the 300 year control integration have been analyzed. The annual cycles of wind stress, current transports, and SST associated with the Brazil-Malvinas confluence region compare quite well to observations. This is a significant achievement because the CSM is a coupled model, and comparing well to ocean observations is considerably more difficult to achieve than with an ocean model alone forced by observations.

A coarse resolution model, such as the CSM, has successfully reproduced major features of the BMC seasonality, because both the amplitudes and phases of the Brazil and Malvinas Current annual cycles are comparable to observations. However, the seasonal movement of the BMC separation point is much smaller in the model, because the local dynamics involving recirculation and meander dynamics are not resolved. It was found that the CSM exhibits a strong correlation between the extremes of the annual cycle for both transport and wind stress curl at 40°S. CSM current transports are quite close to observations, and near 38°S they are consistent with transport estimates from hydrographic data. In the CSM this seasonal variation in transport is in phase with variations in the local wind stress.

The latitudinal displacement of the 24°C and 17°C isotherms between austral summer and winter was shown to have a range of 20° and 12°, respectively, in both the CSM and the *Reynolds* and *Smith* [1994] climatology. Not only the magnitude of the north-south displacement is comparable to observations, but also its phase throughout the year: northward during austral winter and southward during austral summer.

Although this study focused on the seasonal cycle of the southwest Atlantic and BMC circulation, it should be noted that there is substantial variability at interannual and lower frequencies in this coupled simulation. Understanding and assessing its impact on regional climate in southern South America is the subject of ongoing research.

Acknowledgments. This work was supported in part by grants FAPESP-98/13397-4 and CNPq-300223/93-5. Additional travel support was provided to I.W. by the Climate and Global Dynamics Division at NCAR. NCAR is funded by the National Science Foundation. I.W. thanks Steve Hankin and the FERRET support group for the graphics.

References

Agra, C., and D. Nof, Collision and separation of boundary currents, *Deep Sea Res.*, 40, 2259-2282, 1993.

Bonan, G., The land surface climatology of the NCAR Land Surface Model Coupled to the NCAR Community Climate Model, *J. Clim.*, 11, 1307-1326, 1998.

Boville, B., and P. R. Gent, The NCAR Climate System Model, Version One, *J. Clim.*, 11, 1115-1130, 1998.

Chelton, D. B., M. G. Schlax, D. L. Witter, and J. G. Richman, Geosat altimeter observations of the surface circulation of the Southern Ocean, *J. Geophys. Res.*, 95, 17877-17903, 1990.

Ciotti, A. M., C. Odebrecht, G. Fillmann, and O. O. Moller Jr, Freshwater outflow and Subtropical Convergence influence on phytoplankton biomass on the southern Brazilian continental shelf, *Cont. Shelf Res.*, 15(14), 1737-1756, 1995.

Confluence Principal Investigators, Confluence 1988-1990: An intensive study of the southwestern Atlantic, *Eos Trans. AGU*, 71(41), 1131-1133 and 1137, 1990.

Danabasoglu, G., On the wind-driven circulation of the uncoupled and coupled NCAR Climate System Ocean Model, *J. Clim.*, 11, 1442-1454, 1988.

Da Silva, A., A. Young, and S. Levitus, Atlas of Surface Marine Data 1994, v. 1, *Algorithms and Procedures*, NOAA Atlas NESDIS 6, U.S. Dep. of Commer., Washington, D.C., 1994.

Flato, G. M., and W. D. Hibler, Modeling ice pack as a cavitating fluid, *J. Phys. Oceanogr.*, 22, 626-651, 1992.

Gan, J. P., L. A. Mysak, and D. N. Straub, Simulation of the South Atlantic Ocean circulation and its seasonal variability, *J. Geophys. Res.*, 103, 10,241-10,251, 1998.

Garzoli, S. L., Geostrophic velocity and transport variability in the Brazil-Malvinas confluence, *Deep Sea Res.*, 40, 1379-1403, 1993.

Garzoli, S. L., and Z. Garraffo, Transports, frontal motions and eddies at the Brazil-Malvinas Currents confluence, *Deep Sea Res.*, 36, 681-703, 1989.

Garzoli. S. L., and C. Giulivi, What forces the variability of the southwestern Atlantic boundary currents?, *Deep Sea Res.*, 41, 1527-1550, 1994.

Garzoli, S. L., and C. Simonato, Baroclinic instabilities and forced oscillations in the Brazil / Malvinas confluence front, *Deep Sea Res.*, 37, 1053-1074, 1990.

Gent, P., F. Bryan, G. Danabasoglu, S. Doney, W. Holland, W. Large, and J. C. McWilliams, The NCAR Climate System Model global ocean component, *J. Clim.*, 11, 1287-1306, 1998.

Goni, G., S. Kamholz, S. Garzoli, and D. Olson, The Brazil-Malvinas confluence based on inverted echo sounders and altimetry, *J. Geophys, Res.*, 101, 16,273-16,289, 1996.

Gordon, A. L., Brazil-Malvinas confluence - 1984, *Deep Sea Res.*, 36, 359-384, 1989.

Gordon, A. L., and C. L. Greengrove, Geostrophic circulation of the Brazil-Falkland confluence, *Deep Sea Res.*, 33, 573-585, 1986.

Hack, J. J., J. T. Kiehl, and J. Hurrell, The hydrologic and thermodynamic characteristics of the NCAR CCM3, *J. Clim.*, 11, 1179-1206, 1998.

Hellerman, S., and M. Rosenstein, Normal monthly wind stress over the world ocean with error estimates, *J. Phys. Oceanogr.*, 13, 1093-1104, 1983.

Kalnay, E., et al., The NCEP/NCAR 40-year reanalysis project, *Bull. Am. Meteorol. Soc.*, 77, 437-471, 1996.

Kiehl, J. T., J. J. Hack, G. Bonan, B. A. Boville, D. Williamson, and P. Rasch, The National Center for Atmospheric Research Community Climate Model: CCM3, *J. Clim.*, 11, 1131-1149, 1998.

Legeckis, R. V., and A. L. Gordon, Satellite observations of the Brazil and Falkland Currents - 1974 to 1976 and 1978, *Deep Sea Res.*, 29, 375-401, 1982.

Maamaatuaiahutapu, K., V. C. Garçon, C. Provost, M. Boulahdid, and A. P. Osiroff, Brazil-Malvinas confluence: Water mass composition, *J. Geophys. Res.*, 97, 9493 - 9506, 1992.

Matano, R. P., On the separation of the Brazil Current from the coast, *J. Phys. Oceanogr.*, 23, 79-90, 1993.

Matano, R. P., M. G. Schlax, and D. B. Chelton, Seasonal variability in the southwestern Atlantic, *J. Geophys. Res.*, 98, 18,027-18,035, 1993.

Oberhuber, J., An atlas based on COADS data set, *Tech. Rep.* 15, Max-Planck-Inst. fur Meteorol., 1988.

Olson, D. B., G. P. Podesta, R. H. Evans, and O. B. Brown, Temporal variations in the separation of Brazil and Malvinas Currents, *Deep Sea Res.*, 35, 1971-1990, 1988.

Peterson, R. G., The boundary currents in the western Argentine Basin, *Deep Sea Res.*, 39, 623-644, 1992.

Peterson, R. G., and L. Stramma, Upper-level circulation in the South Atlantic, *Prog. Oceanogr.*, 26, 1-73, 1991.

Provost, C., O. Garcia, and V. Garçon, Analysis of sea surface temperature time series in the Brazil-Malvinas Currents confluence region: Dominance of the annual and semiannual periods, *J. Geophys. Res.*, 97, 17,841 - 17,858, 1992.

Reid, J. L., On the total geostrophic circulation of the South Atlantic Ocean: Flow patterns, tracers and transports, *Prog. Oceanogr.*, 23, 149-244, 1989.

Reynolds, R. W., and T. M. Smith, A high resolution global sea

surface temperature climatology, *J. Clim.*, 7, 929-948, 1994.

Roden, G. I., Thermohaline fronts and baroclinic flow in the Argentine Basin during the austral spring of 1984, *J. Geophys. Res.*, 91, 5075 -5093, 1986.

Slutz, R. J., S. J. Lubker, J. D. Hiscox, S. D. Woodruff, R. L. Jenne, D. H. Joseph, P. M. Steuer, and J. D. Elms, *Comprehensive Ocean-Atmosphere Data Set: Release 1*, 268 pp., NOAA Environ. Res. Lab., Boulder, Colo., 1985.

Smith, L. T., E. P. Chassignet, and D. Olson, Wind-forced variations in the Brazil-Malvinas confluence region as simulated in a coarse resolution numerical model of the South Atlantic, *J. Geophys. Res.*, 99, 5095-5177, 1994.

Veronis, G., Model of world ocean circulation, I, Wind-driven, two-layer, *J. Mar. Res.*, 31, 228-288, 1973.

Weatherly, J. W., B. P. Briegleb, W. G. Large, and J. A. Maslanik, Sea ice and polar climate in the NCAR CSM, *J. Clim.*, 11, 1472-1486, 1998.

Woodruff, S. D., R. J. Slutz, R. L. Jenne, and P. M. Steurer, A comprehensive ocean-atmosphere data set, *Bull. Am. Meteorol. Soc.*, 68, 1239-1250, 1987.

I Wainer, Department of Physical Oceanography, University of São Paulo, Praça do Oceanográfico 191, São Paulo, 05508-900, Brazil. (wainer@usp.br)

P. Gent, National Center for Atmospheric Research, P. O. Box 3000, Boulder, CO 80307, USA.

G. Goni, U.S. Atlantic Oceanographic and Meteorological Laboratory, National Oceanic and Atmospheric Administration, U.S. Department of Commerce, Miami, FL, USA.

(Received November 16, 1999; revised April 10, 2000; accepted May 12, 2000)